

**Figure 2.** Relationship between the molecular dimensions of a surfactant monomer and the packing parameter ( $P$ ) for packing in a normal bilayer (left) and in a special (see text) interdigitated bilayer (right).

the bilayer are known. However, we favor the second explanation, since the presence of the hydrophilic ester group will probably induce an increase of the headgroup area, facilitating interdigitation, rather than a decrease of the headgroup area.

### Conclusions

The results described in this paper indicate that the morphology of a surfactant aggregate is mainly determined by the shape of the surfactant monomer. This dependence can be quantified by the packing parameter approach, as suggested by Israelachvili<sup>10</sup> for linear compounds. However, a novel combination of the approach of Israelachvili

with the ladder model is necessary to understand the dependence of the aggregate type on the surfactant concentration. Thus, in summary: surfactants with  $P \leq 1/3$  associate into spherical micelles that do not grow upon increasing surfactant concentration; surfactants with  $1/3 < P \leq 1/2$  associate into spherical micelles that grow upon increasing surfactant concentration; and surfactants with  $1/2 < P \leq 1$  aggregate into bilayers. The morphology of the aggregate does not depend on the alkyl chain length ( $n_c$ ), although the thermodynamic stability of the aggregate is affected. The dependence of the  $l_c$  on  $n_c$  solely originates from the dependence of the aggregation number of the spherical micelle on  $n_c$ .

The possibility for backfolding determines the morphology of the aggregate in cases where the headgroup substituent (1-alkyl chain) is varied and the 4-alkyl chain is kept constant (*n*-dodecyl). Preferential bilayer formation is found when backfolding occurs; otherwise spherical micelles are formed that grow into rodlike micelles at increasing surfactant concentrations.

Surfactants associate into bilayers instead of micelles when an ester group is inserted between the unbranched 4-alkyl chain and the pyridinium ring. Interdigitated packing of the alkyl chains, resulting in a change of the geometrical constraints for packing into a bilayer, is probably the origin for this remarkable aggregation behavior for an unbranched, single-chain surfactant.

**Acknowledgment.** The investigations were supported by the Netherlands Foundation for Chemical Research (SON) with financial aid from the Netherlands Foundation for Scientific Research (NWO). We thank Dr. M. Veenhuis and J. Zagers of the Biological Centre and J. F. L. van Bremen of the Biochemistry Department for the EM measurements.

## Mechanisms of Macrocyclization. The Condensation of Resorcinol with Aldehydes<sup>1</sup>

Frank Weinelt\*<sup>†</sup> and Hans-Jörg Schneider\*<sup>‡</sup>

Fachrichtung Organische Chemie der Universität des Saarlandes, D-6600 Saarbrücken 11, and Sektion Chemie der Karl-Marx-Universität, Leipzig, Germany

Received December 11, 1990

The title reactions proceed in high yields without high dilution techniques as long as substituents allow hydrogen bonds between the phenolic units and do not lead to steric hindrance. Isomerization rates for three epimeric cyclophanes, including a hitherto undiscovered one, are obtained by least-squares fit with integrated rate equations. The buildup sequences of oligomers, polymers, and macrocycles are analyzed by numerical stepwise integration with 50 rate constants, based on the fit of time-concentration curves of seven identified structures that were followed by proton NMR. Macrocyclization is favored by the following: (a) fast degradation of oligomers, (b) fast ring closure of tetramers, as well as (c) fast chain growth to these in comparison to ring opening. Homogeneous reaction conditions, here with methanol as solvent, are essential not only for the quantitative analyses, but also for the solubility of polymers in view of their degradation and for the observation of new stereoisomers. Molecular mechanics calculations with the CHARMM field and model considerations identify the factors responsible for the unique preference for cyclization over polymerization. Both hydrogen bonds between the phenolic units and 1.5 interactions between phenolic groups and the methyl substituent—stemming from the acetaldehyde—strongly favor folded conformers with small distances around  $d = 3.3\text{--}4.6$  Å between the terminal reacting centers in comparison to stretched conformations with  $d = 12.2\text{--}18.3$  Å.

The development of supramolecular chemistry and in particular its practical application depends to a considerable degree on the synthetic availability of macrocyclic host compounds in sufficient quantities. In spite of im-

pressive recent advances,<sup>2</sup> the preparation of such macrocycles often requires application of high dilution prin-

\*Karl-Marx-Universität (present address: Hoechst AG, D-W 8269 Burgkirchen 2, FRG).

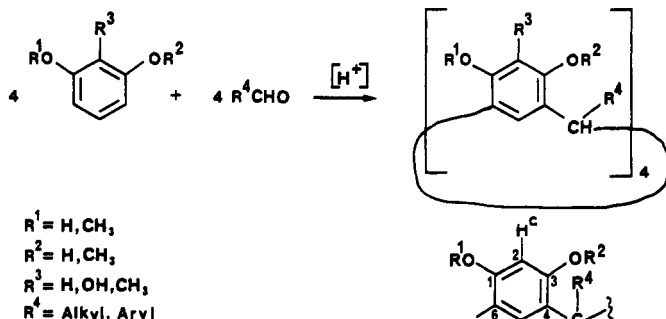
<sup>†</sup>Universität der Saarlandes.

(1) Part 27 of the Saarbrücken series in Host-Guest chemistry. Part 26: Schneider, H.-J. et al. In *Frontiers in Supramolecular Chemistry and Photochemistry*; Schneider, H.-J., Dürr, H., Eds.; VCH: Weinheim, 1991. (2) (a) Stoddart, J. F. In *Frontiers in Supramolecular Organic Chemistry and Photochemistry*; Schneider, H.-J.; Dürr, H., Eds.; Verlag Chemie: Weinheim, 1991.

**Table I. Cyclophanes from the Condensation of Different Aldehydes with Resorcinol and Its Methyl Ethers<sup>a</sup>**

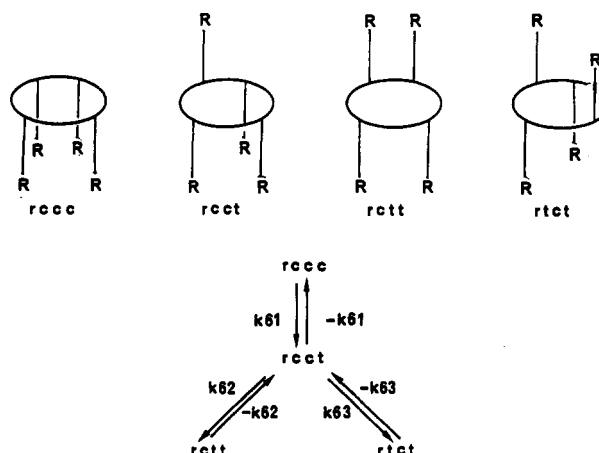
R <sup>1</sup>	R <sup>2</sup>	R <sup>3</sup>	R <sup>4</sup>	yield <sup>b</sup> (%)	rccc (%)	rcct	rctt
H	H	H	CH <sub>3</sub>	88	2a (50)	2b 40%	2c (10)
H	CH <sub>3</sub>	H	CH <sub>3</sub>	2 <sup>c</sup>	3a		
CH <sub>3</sub>	CH <sub>3</sub>	H	CH <sub>3</sub>	0.2 <sup>d</sup>	4a		
H	H	OH	CH <sub>3</sub>	64	5a (62)		5c (38)
H	H	COOH	CH <sub>3</sub>	0 (<1)			
H	H	H	Ph	90	6a (38)		6c (62)
H	H	H	2-OH-Ph	78	7a (33)		7c (67)
H	H	H	4-OH-Ph	91	8a (70)		8c (30)
H	H	H	4-CH <sub>3</sub> -Ph	94			9c
H	H	H	2,4,6-CH <sub>3</sub> -Ph	0 (<1)			
H	H	H	3-NO <sub>2</sub> -Ph	72 <sup>e</sup>	10a (87)		10c (13)

<sup>a</sup> Reaction conditions: 5% solution of hydrogenchloride in methanol at 65 °C; concentration of educts, 1 mol/L; reaction time, 1 h, unless noted otherwise. Isomer ratios were determined by <sup>1</sup>H NMR signal integration (for 2 and 5, CH<sub>3</sub> signals; for 6–8 and 10, Ph-CH signals. R<sup>1</sup> to R<sup>4</sup>: see Scheme I, isomers rccc, rcct, rctt see Scheme II and Figure 2. <sup>b</sup> Isolated as mixture of isomers. <sup>c</sup> Total cyclic product 17% (by HPLC). <sup>d</sup> Total cyclic products <1% (by HPLC) [Educts] 1.85 mol/L; reaction time, 5 h.

**Scheme I. Reaction of Resorcinol Derivatives with Aldehydes (with C and H Numbering)**

ciples in order to diminish polymerization, frequently with the consequence of subgram quantities within several days and of large amounts of pure and expensive and/or toxic solvents.<sup>3</sup> Condensation products from phenols and aldehydes,<sup>4</sup> which are also of increasing interest for technical applications<sup>4c,5</sup> beyond host-guest chemistry, are well-known exceptions: they are usually obtained in high yields without dilution techniques, partially even in aqueous or protic solvents. The present paper addresses the question why and under which conditions the synthesis of such macrocycles can proceed in a predictable way, including the quite variable stereochemistry of the products.

After the first investigation by A. von Baeyer in 1872, the acid-catalyzed condensation of resorcinol with alkyl or aryl aldehydes (Scheme I) has been the subject of numerous papers.<sup>6</sup> Whereas the formation of calixarenes from 4-alkyl phenols and formaldehyde under basic con-

**Scheme II. Stereoisomers of the Macrocycles and Their Isomerization Pathways**

ditions is largely a function of alkali metal template as well as of solubility effects,<sup>4</sup> the resorcinol reactions usually lead in high yield only to metacyclophanes containing invariably four phenyl rings. The presence of the alkyl or aryl substituents R from the aldehydes interestingly allows the formation of four stereoisomers (Scheme II), designated rccc, rctt, rcct, and rtct. Configurations and conformations of some of these isomers have been the subject of earlier investigations,<sup>6c–e,1</sup> also by the Leipzig group.<sup>7</sup> Until now, however, only the rccc and rctt epimers from the acetaldehyde reaction have been described.<sup>6,7</sup> The Saarbrücken group has shown that the corresponding tetraphenolates can act as very strong receptors for choline and related ammonium compounds;<sup>8</sup> Cram et al.<sup>9</sup> have used the rccc isomers as the synthetic basis for the construction of a whole new host class. The application of methanol as solvent and the thus possible homogeneous reaction conditions allow not only the study of the kinetics and thermodynamics of the condensations with resorcinol and acetaldehyde but also the observation of an until now missing stereoisomer in high yields.

### Experimental Results

The scope of the reaction, which is efficiently catalyzed by any mineral acid in water or alcohol, is limited only by

(3) (a) Rossa, L.; Vögtle, F. *Top. Curr. Chem.* 1983, 113, 1. (b) *Synthesis of Macrocycles*; Izatt, R. M., Christensen, J. J., Eds.; Wiley: New York, 1987. (c) Lindoy, L. F. *The Chemistry of Macrocyclic Ligand Complexes*; Cambridge University Press: Cambridge, 1989.

(4) (a) Gutsche, C. D. *Acc. Chem. Res.* 1983, 16, 161. (b) Gutsche, C. D. *Top. Curr. Chem.* 1984, 123, 1. (c) Gutsche, C. D. ref 3a, p. 93. (d) Dhawan, B.; Chen, S.-I.; Gutsche, C. D. *Makromol. Chem.* 1987, 188, 921.

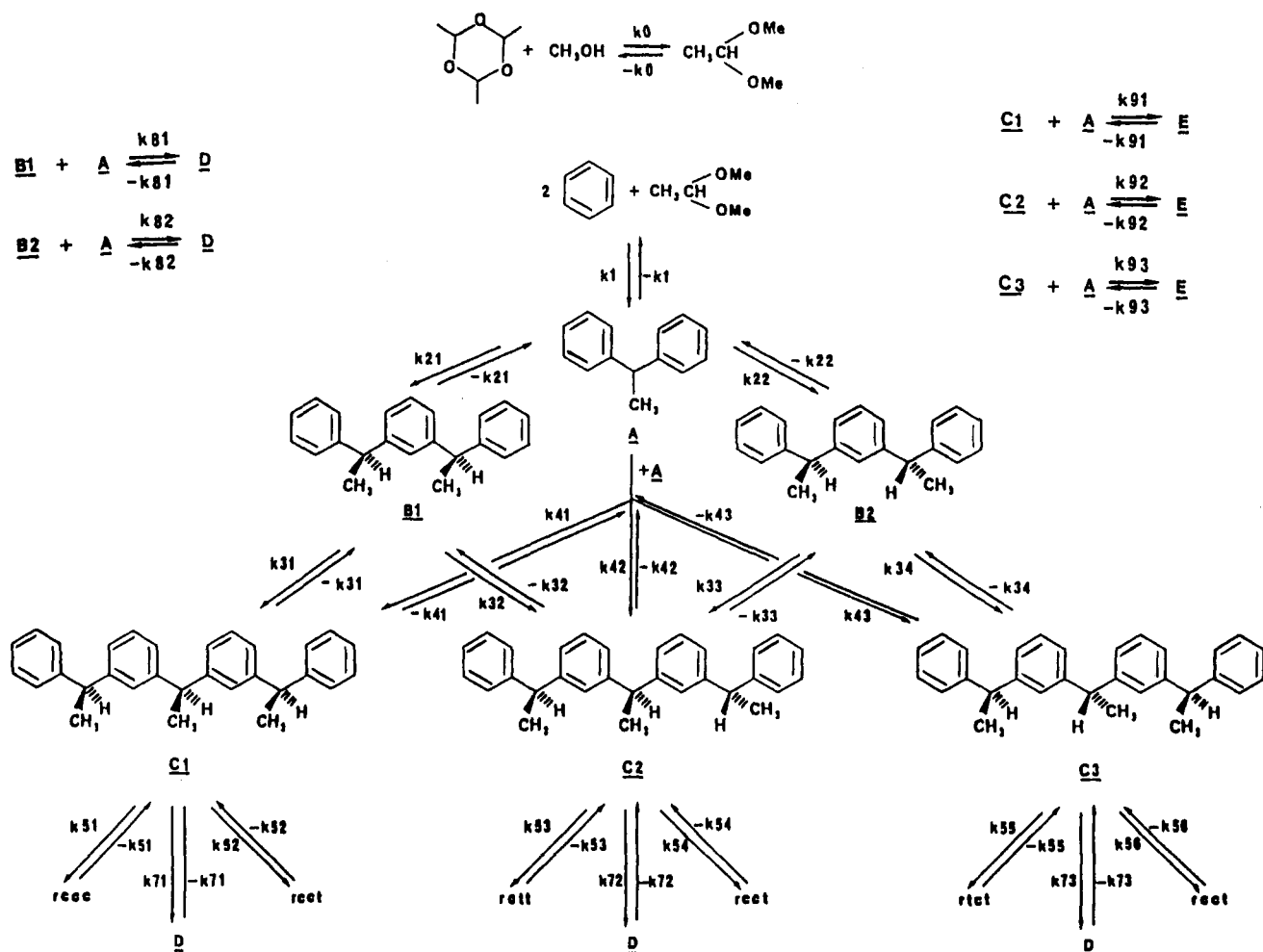
(5) The resorcinol-derived cyclophanes are excellent antioxidants, e.g., for rubber, and have a remarkably low toxicity: patent application DDR-WP CO7/c 335784/8, December 12, 1989.

(6) (a) Baeyer, A. v. *Ber. Dtsch. Chem. Ges.* 1872, 5, 25. (b) Niederl, J. B.; Vogel, H. J. *J. Am. Chem. Soc.* 1940, 62, 2512. (c) Zinke, A.; Ziegler, E. *Ber. Dtsch. Chem. Ges.* 1944, 77, 284. Zinke, A.; Ott, R.; Garanna, F. *H. Monatsh. Chem.* 1958, 89, 135. Zinke, A.; Kretz, R.; Leggewie, E.; Hössinger, K. *Monatsh. Chem.* 1952, 83, 1213. (d) Erdtman, H.; Haglid, F.; Ryhage, R. *Acta Chem. Scand.* 1964, 18, 1249. Erdtman, H.; Högberg, A. G. S.; Abrahamson, S.; Nilsson, B. *Tetrahedron Lett.* 1968, 1679. (e) Högberg, A. G. S. *J. Org. Chem.* 1980, 45, 4498. (f) Högberg, A. G. S. *J. Am. Chem. Soc.* 1980, 102, 6046. (g) Nilsson, B. *Acta Chem. Scand.* 1968, 22, 732. (h) Palmer, K. J.; Wong, R. Y.; Jurd, L.; Stevens, K. *Acta Cryst.* 1976, 32B, 847. (i) Abis, L.; Dalcanele, E.; Du Voxel, A.; Spera, S. *J. Org. Chem.* 1988, 53, 5475 and references cited in these papers.

(7) Mann, G.; Weinelt, F.; Hauptmann, S. *J. Phys. Org. Chem.* 1989, 2, 531.

(8) Schneider, H.-J.; Güttes, D.; Schneider, U. *J. Am. Chem. Soc.* 1988, 110, 6449 and references cited therein.

(9) (a) Tucker, J. A.; Knobler, C. B.; Trueblood, K. N.; Cram, D. J. *J. Am. Chem. Soc.* 1989, 111, 3688. (b) Bryant, J. A.; Ericson, J. L.; Cram, D. J. *Ibid.* 1990, 112, 1255 and references cited therein.

Scheme III. Buildup Sequence of Oligomers and Macrocycles with Corresponding Rate Constants  $k$ . Resorcinol Units Are Represented by Hexagons; D, "Pentamers" (Five Resorcinol Units); E, "Hexamers" (Six Units)

steric hindrance, e.g., with mesityl aldehyde and by factors that influence the possibility of hydrogen bond formation between the phenolic OH groups of adjacent resorcinol units (Table I). This is evident from the strong decrease in macrocycle formation with etherification of resorcinol as well as with additional OH substituents in the vicinity to the phenolic groups (Table I), although steric hindrance can also contribute to the effects. The role of the hydrogen bonds will be discussed in the following text in detail on the basis of force field calculation results.

The buildup of oligomers and rings could be followed quantitatively by high-field  $^1\text{H}$  NMR spectroscopy, although aromatic signals were only partially assigned due to heavy overlap in the analyzed mixtures. HPLC separations on reversed-phase columns led only to partial separations of the stereoisomers B1 and B2 (Scheme III) from other oligomers, but did corroborate the NMR analyses with respect to the other structures. The electrophilic species attacking resorcinol in methanol stems not directly from the aldehyde but from its rapidly formed dimethyl acetal. We then could identify and measure six different compounds designated in Scheme III as A, the first observable intermediate, B1 and B2, the subsequently generated diastereomers, and three epimeric cyclophanes. The "tetrameric" precursors C1, C2, and C3 cyclize too fast to accumulate in observable quantities; the intensities of the corresponding NMR signal are in addition decreased by lower symmetry in comparison, e.g., to the cyclophanes. Higher oligomers such as D or E were present as unidentified multicomponents in concentrations of up to 45%

(Table I\*, supplementary material) together with C at intermediate reaction times, but largely disappeared toward the end due to back reactions to C and from there on to the macrocycles. These findings were substantiated by the kinetics of the reaction (see the following text). All observed intermediates by NMR showed resorcinol and not hydroxyethyl units at the terminal positions, which is in accord with the fast reaction of such benzhydrols under acidic conditions.<sup>10</sup>

While the *rtct* stereoisomer still escaped positive identification due to its minor contribution, the *rcct* epimer was unequivocally assigned for the first time on the basis of its NMR spectra, and in fact predominates in equilibration experiments (Figure 1). We assume that it had been overlooked until now due to its minor formation ( $\leq 10\%$ ) in aqueous and heterogeneous solution. Equilibration experiments with the pure *rcct* form showed only the additional *rtct* and *rcct* isomers. A computer fit (Figure 1) of the measured time dependencies on the basis of integrated rate equations<sup>11</sup> furnished rate constants for the isomerizations, which all must proceed via the *rcct* epimer (Scheme II). Temperature increases showed small but distinct differential effects on rate and equilibrium constants (Table II) and point to small enthalpy advantages for the *rcct* isomer. Figure 2 illustrates configuration

(10) Hultsch, K. *Chemie der Phenolharze*; Springer Verlag: Berlin, 1950.

(11) Frost, A. A.; Pearson, R. G. *Kinetik und Mechanismen homogener chemischer Reaktionen*; VCH: Weinheim, 1964.

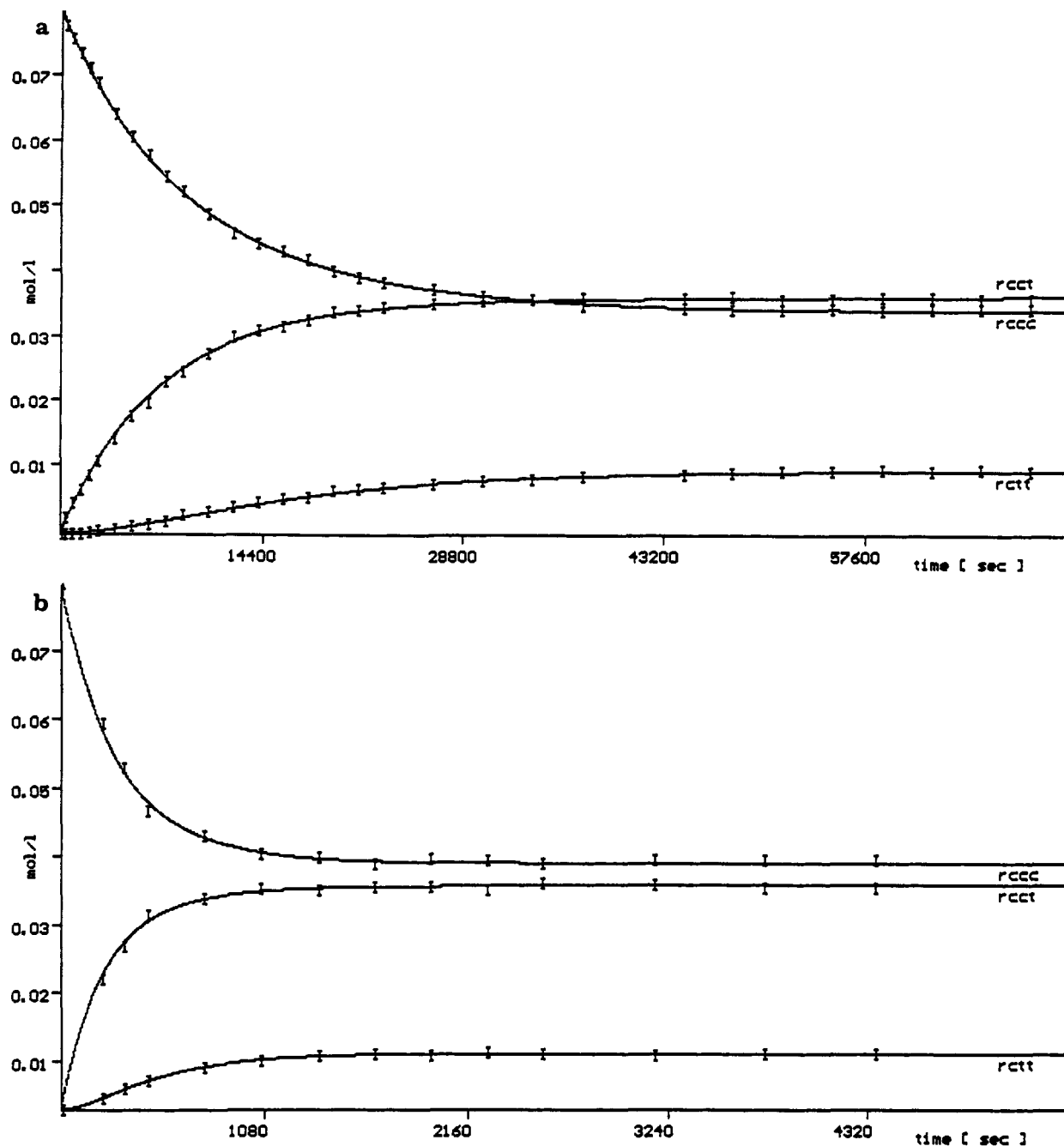


Figure 1. Time-concentration curves for the isomerizations (a) at 300 K and (b) at 323 K (experimental points I and computer-fitted curves).

and possible conformation of the stereoisomers.

The kinetic analysis of the complete buildup reactions had to encompass at least 50 single rate constants  $k$  (Scheme III), although immediately connected steps such as water elimination from the hydroxyethyl product and electrophilic substitution were described by *one* rate-determining constant for each intermediate or product. An approximate solution for the differential rate equations thus involved was achieved by numerical integration and approximate fit to the observed time-concentration curves (Figure 3), based on a computer program that varied starting  $k$  values stepwise in a grid procedure; only the isomerization velocities were taken from the explicit kinetic analysis described previously. Although the multiparameter fit thus achieved is only approximate, the set of best rate constants (Table III) is chemically reasonable in terms of chemically comparable steps for the reactions. The most important features are that (a) chain growth is faster than

Table II. Isomerization of the Cyclophanes: Kinetic and Thermodynamic Data<sup>a</sup>

		$\Delta H^*$	$\Delta S^*$	$k_{300K} \times 10^5$	$k_{323K} \times 10^5$	
rccc	rcct	$k_{61}$	$114 \pm 10$	55	6.56	1.86
rcct	rccc	$-k_{61}$	$119 \pm 10$	70	6.14	2.04
rcct	rctt	$k_{62}$	$126 \pm 7$	85	2.50	0.84
rctt	rcct	$-k_{62}$	$129 \pm 8$	110	9.31	3.39
		in equilibrium <sup>b</sup>	300 K (%)	323 K (%)		
		rccc	43	47		
		rcct	45	42		
		rctt	12	11		
		$\Delta G^\circ$ rccc $\rightarrow$ rcct <sup>c</sup>	-0.11	0.30		
		$\Delta G^\circ$ rcct $\rightarrow$ rctt <sup>c</sup>	3.3	3.6		

<sup>a</sup>  $\Delta H$ ,  $\Delta G$  in kJ/mol;  $\Delta S^*$  in  $J K^{-1} mol^{-1}$  ( $\pm 35$  average error); rate constants  $k$  in  $[s^{-1}]$ ; temp in K ( $\pm 1$  K). <sup>b</sup> Determined after 10 half-life times on the average. <sup>c</sup> From kinetic data. All measurements starting with pure rccc in  $CD_3OD$  with 1.45 N HCl.  $\Delta H^*$ ,  $\Delta S^*$  from Eyring plots with  $k$  from three other temperatures (308, 313, 318 K).

**Table III. Rate Constants for Scheme III from Fit to the Observed Time-Concentration Curves (Figure 1)<sup>a</sup>**

$k_0 = 0.0005$			
$-k_0 = 0.0001$			
$k_1 = 0.1$	$-k_1 = 0$		
$k_{21} = 0.3$	$-k_{21} = 5e^{-4}$	$k_{22} = 0.07$	$-k_{22} = 8e^{-4}$
$k_{31} = 0.8$	$-k_{31} = 1e^{-4}$	$k_{32} = 0.4$	$-k_{32} = 1e^{-4}$
$k_{33} = 0.6$	$-k_{33} = 1e^{-5}$	$k_{34} = 0.6$	$-k_{34} = 1e^{-5}$
$k_{41} = 0.1$	$-k_{41} = 4e^{-5}$	$k_{42} = 0.09$	$-k_{42} = 4e^{-5}$
$k_{43} = 0.04$	$-k_{43} = 4e^{-5}$		
$k_{51} = 0.005$	$-k_{51} = 2e^{-5}$	$k_{52} = 0.007$	$-k_{52} = 5e^{-6}$
$k_{53} = 0.009$	$-k_{53} = 5e^{-6}$	$k_{54} = 0.007$	$-k_{54} = 5e^{-6}$
$k_{55} = 0.001$	$-k_{55} = 1e^{-5}$	$k_{56} = 0.007$	$-k_{56} = 5e^{-6}$
$k_{61} = 6.1e^{-5}$	$-k_{61} = 6.6e^{-5}$	$k_{62} = 2.5e^{-5}$	$-k_{62} = 9.3e^{-5}$
$k_{63} = 0$	$-k_{63} = 9e^{-5}$		
$k_{71} = k_{72} = k_{73} = 0.05$	$-k_{71} = -k_{72} = -k_{73} = 1e^{-5}$		
$k_{91} = k_{92} = k_{93} = 0.15$	$-k_{91} = -k_{92} = -k_{93} = 5e^{-4}$		

<sup>a</sup> In  $s^{-1}$  for first-order reactions, and  $Mol^{-1} s$  for second-order reactions; at  $300 \pm 1$  K in  $CD_3OD$  with 1.45 M HCl.

isomerization of ring structures, whereas degradation (depolymerization) is similar; (b) cyclization rates are faster than ring opening and isomerization; (c) the results require the formation of higher oligomers (D and E), which, however, have degradation rates fast relative to ring opening; and (d) buildup rates of the different diastereomers (B, C, and rings) differ by a factor of up to 4.

The last result already indicates that the ratio of stereoisomers can deviate considerably from the statistically expected ratio, which in the case of the cyclophanes should be  $rccc:rcct:rtcc:rtcc = 2:7:3:2$  if the rate constants for all isomers would be the same. The observed ratio at 300 K is 3.6:3.75:1.0:( $<0.1$ ), slightly changed at 323 K to 4.3:3.8:1.0:( $<0.1$ ).

**Conformations.** The reason for the analytically derived fast cyclizations must be sought for in the conformations of their open-chain precursors. Corresponding acyclic oligomers have been studied experimentally for alkylphenol condensations,<sup>4b</sup> partially even by X-ray crystallography. However, no kinetic analyses were reported until now, and it is difficult to derive conclusions with respect to the reacting conformers, which must obviously bend prior to ring closure in conformations described earlier by the term "pseudocalixarene".<sup>4b</sup>

It was hoped that molecular mechanics calculations not only would predict the conformations responsible for the cyclization but also would help to factorize the interactions leading to the unique preference for ring closure over polymerization. With the aid of the CHARMM force field<sup>12</sup> the open-chain "tetramer" with the  $R^*,R^*,R^*$  configuration (Scheme III) as precursor of the rccc ring was subject to energy minimizations. Extensive use of different starting conformations with a wide range of torsions led to nine distinct optimized structures; they are grouped in Table IV in stretched and folded forms and characterized by the distance  $d$  between the C-OH carbon atom and the C-6 of the electrophilically attacked terminal resorcinol ring. The striking result is that all stretched conformers (Table IV, T1-T6) with  $d = 12-18$  Å have total energies that are 3-13 kcal/mol higher than those of the folded counterparts (T7-T9 in Table IV) with  $d = 3.3-4.3$  Å.

The high stability of the folded pseudocalixarene-like structures is first the consequence of their better ability to form hydrogen bonds between the phenolic hydroxyls

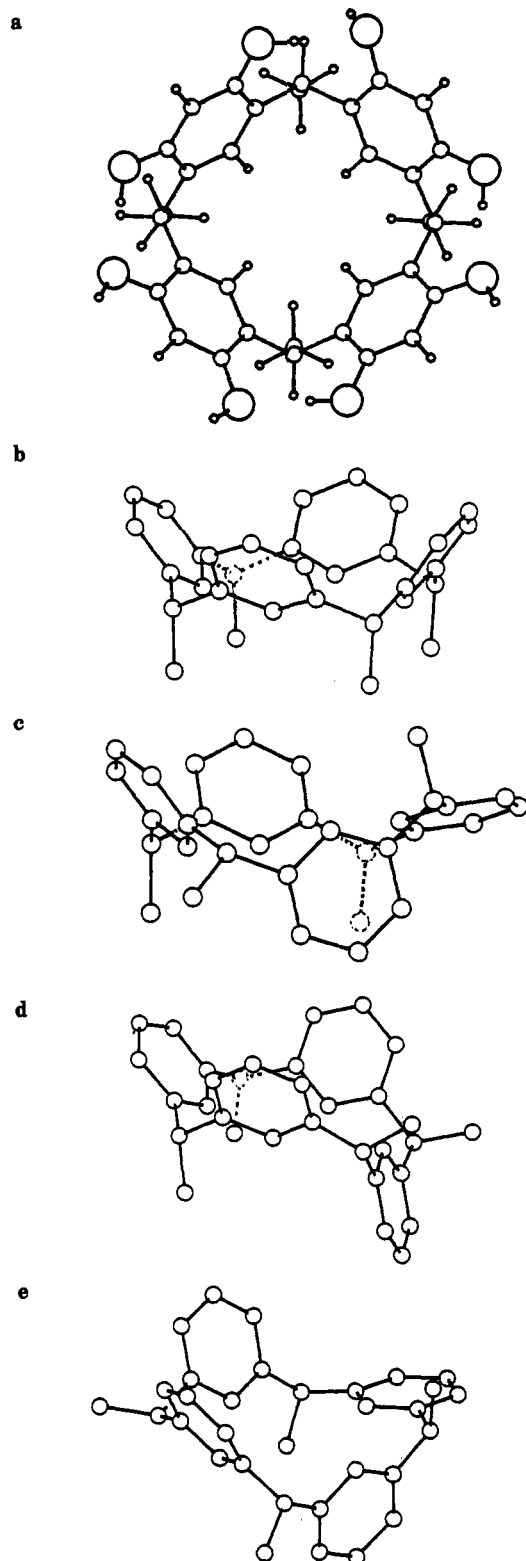


**Figure 2.** Optimized geometries for the macrocyclic stereoisomers: a, rccc, top view; b, rccc; c, rcct; d, rcct; e, rtcc (b-e side views, for the sake of clarity H and O atoms omitted).

of adjacent resorcinol units, which appear bifurcated in all simulations. The average contribution per single hydrogen bond ranges between 1.3 and 2.0 kcal/mol. The systems were simulated in a gas-like environment, and one might expect that the presence of excess water and/or methanol as solvent should compete efficiently with the intramolecular phenolic hydrogen bonds. On the other hand, inspection of the computer-generated models as well as a tentative simulation of rccc within a waterbox shows

(12) See, for example: Brooks, C. L.; Karplus, M. In *Methods of Enzymology*; Academic Press: New York, 1986; Vol. 127 p 369 ff.

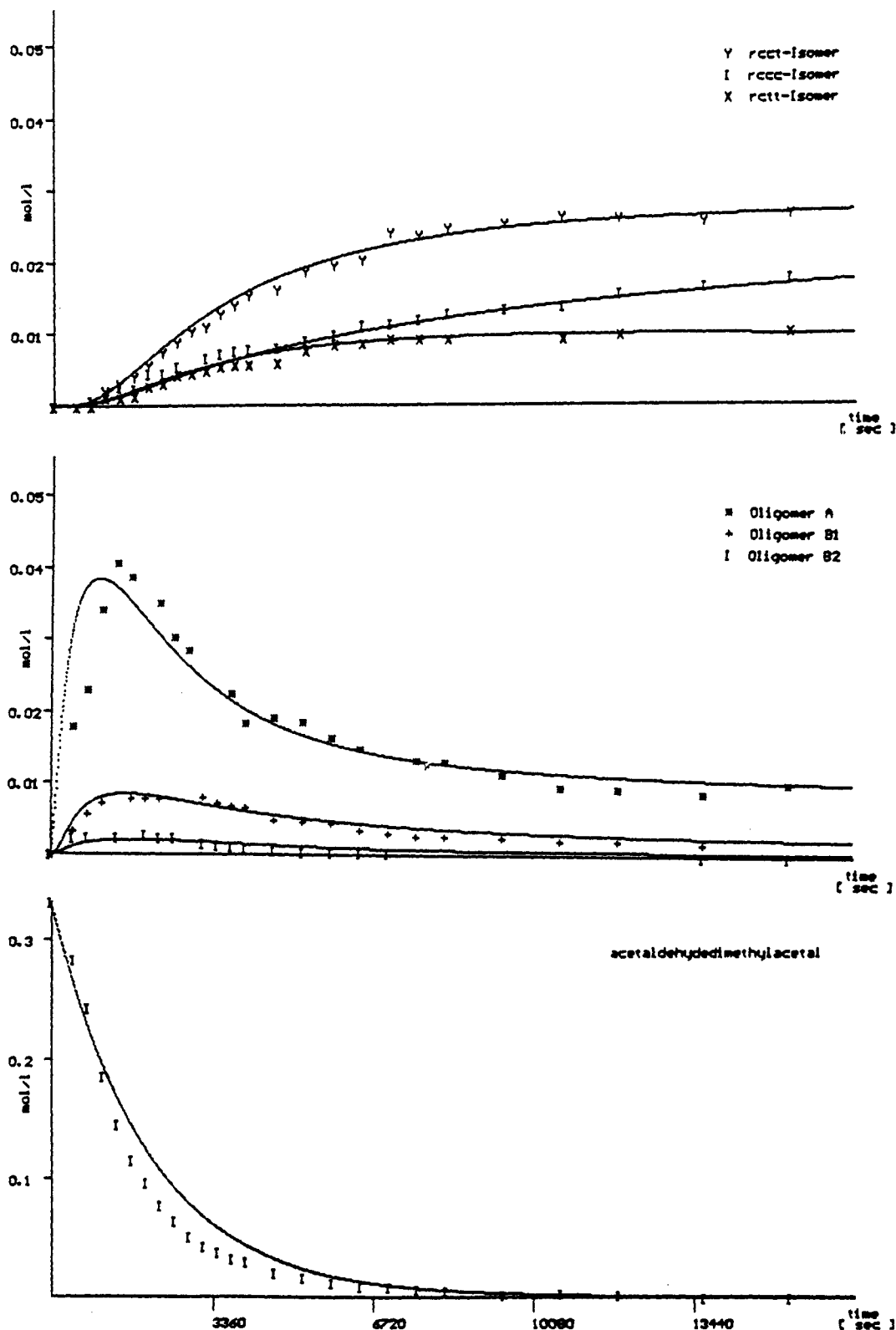


Figure 3. Time-concentration curves for the buildup of oligomers A, B1, and B2, macrocycles rccc, rccr, and rctt, and the disappearance of aldehyde acetal.

that water molecules could be inserted between the phenolic hydroxyls only at the expense of substantial strain built up in the chains. This situation is reminiscent of hydrogen bonds in cyclodextrins, where interference of water is also excluded by the vicinity of interglucose hydroxyl groups. Furthermore, CHARMM simulations with suppressed hydrogen bonds also show folded conformers as more stable in agreement with the generally lower contributions of van der Waals and even bond angle strain

from the calculations including H-bond potentials. Consequently, additional factors to the phenolic hydrogen bonds should also contribute to the enhanced tendency for cyclization.

A closer inspection of molecular models and computer generated structures reveals a more detailed insight to the factors stabilizing folded conformers. The basic features of diphenylmethane conformations have been discussed thoroughly, e.g., by Barnes, Mislow et al.,<sup>13</sup> who also sum-

**Table IV. Selected Results from CHARMM Energy Minimizations for Stretched and Folded Tetramer Conformations T1 to T9<sup>a</sup>**

	<i>d</i> (Å)	$\Phi$ m (deg)	total energy	bond angle	coulomb	vdW	H bond	no. of H bonds
T1	18.29	41	-2.68	6.88	-25.67	9.21	<0.0002	0
T2	18.16	41	-1.65	7.29	-25.61	9.42	<0.0002	0
T3	17.61	46	-0.99	7.47	-25.65	9.47	<0.0002	0
T4	16.65	57	-5.43	8.83	-20.87	8.44	-7.95	6
T5	14.42	76	-1.93	6.23	-18.1	5.06	<0.0002	6
T6	12.24	67	-8.32	5.74	-21.14	8.84	-7.99	6
T7	4.57	85	-12.15	5.36	-19.02	6.72	-12.12	6
T8	4.29	92	-13.85	4.71	-23.45	6.90	-8.04	4
T9	3.30	84	-11.25	5.42	-18.51	5.50	-11.68	8

<sup>a</sup> Energies in kcal/Mol; distance *d* between <sup>\*</sup>C(CH<sub>3</sub>)OH and <sup>\*</sup>C6 of the terminal resorcinol unit; gable angle  $\Phi$  as defined in text.

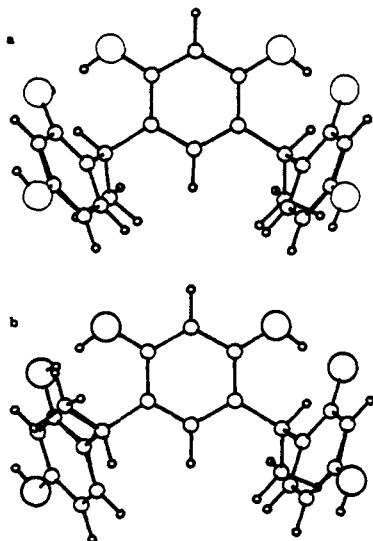


**Figure 4.** Alternative conformations of open-chain precursors, illustrated with the trimer B1 (see Scheme IIIa), see text.

marize earlier investigations in the field. All available evidence points for diphenylmethane itself toward "gable" conformers as the most stable ones, in which the phenyl rings form an angle of  $\Phi = 90^\circ$  with the plane dissecting the H-C-H methylene atoms (compare conformer I or II in Figure 4). Tilting of the phenyl rings to  $\Phi = 30$  or  $40^\circ$  does not enhance the strain considerably, whereas the "perpendicular" structure with one angle of  $\Phi = 0^\circ$  represents the transition state of phenyl ring rotation. Force field and molecular orbital calculations<sup>13</sup> as well as NMR investigations<sup>14</sup> indicate generally small strain differences between all diphenylmethane conformers, which therefore will be determined largely by the additional substituents present in our fragments.

For the sake of brevity we will illustrate the alternative conformations only with one "trimer" as shown in Figure 4. Conformer I is the only one containing exclusively gable structures as well as an ideal disposition for intraphenolic hydrogen bonds. This is visible in all force field simulations of such folded fragments, such as T7-T9 in Table IV, which show gable angles of  $\Phi = 90 \pm 10^\circ$  (Table V\*, supplementary material) as well as O...H...O distances of 2.9 Å, in accord with pertinent literature results.<sup>15</sup> The

"stretched" alternative II, on the other hand, can with gable conformations ( $\Phi = 90 \pm 10^\circ$ ) only produce hydrogen bonds at one side; in addition, it suffers from strong repulsion between the 7-Me group and the 1'-OH substituent. The strain imposed thereby on these stretched conformers is relieved partially by deviations from ideal gable angle and is visible in C4-C7-C6' bond angle deviations (Table V\*, supplementary material). Both the 1.5 repulsion between the phenolic group and the substituent R = CH<sub>3</sub> stemming from the aldehyde as well as the intraphenol-hydrogen bonds are therefore responsible for the unusual fast ring closure in comparison to polymerization.

### Conclusions

The buildup of macrocyclic cavities from small fragments can be followed quantitatively with respect to many intermediates and possible stereoisomeric products. The kinetic and thermodynamic analyses help to define the conditions, under which high yields of macrocyclic products are obtained without high dilution techniques: (1) ring closure is as fast as chain propagation; (2) the macrocyclic products form the thermodynamic sink of the reactions; (3) higher oligomers containing more monomers than required for (1) are degrading (depolymerizing) fast in comparison to the ring opening; and (4) homogeneous reaction conditions are a prerequisite for the sufficiently fast degrading reaction of higher oligomers back to the tetramers and from there to the rings. (In line with this, yields of macrocycles are much lower in aqueous solution at room temperature since the higher oligomers are not soluble under these conditions.)

Simulations with molecular models and force field calculations shed light on the origin of the unique disposition of open chain precursors for ring formation. Folded conformers in which the reacting ends are in vicinity can be stabilized both by substituent repulsion in more stretched open forms as well as by predisposition for intramolecular hydrogen bonds. This is in line with several synthetic observations using other resorcinol derivatives.

### Experimental and Computational Details

<sup>1</sup>H NMR spectra were recorded at 400 MHz with a Bruker AM 400 spectrometer (<sup>1</sup>H) or at 75.4 MHz with a Bruker MSL 300 instrument (<sup>13</sup>C) at ambient temperature. TMS was used as internal reference with  $\delta$  0.00. Mass spectra were recorded on a VG 12-250 instrument. Elemental analyses were performed with a CHO-O-Rapid Heraeus apparatus. Melting points (uncorrected)

(13) See: Barnes, J. C.; Paton, J. D.; Damewood, J. R.; Mislav, K. *J. Org. Chem.* 1981, 46, 4975 and references cited therein.

(14) Schaefer, T.; Niemczura, W.; Danchura, W.; Wildman, T. A. *Can. J. Chem.* 1979, 57, 1881.

(15) (a) Carrns, T.; Eglinton, G. *Nature (London)* 1962, 196, 535. (b) Domenicano, A.; Hargittai, I.; Portalone, G.; Schultz, G. *Acta Chem. Scand.* 1988, A42, 480.

(16) Recent molecular mechanic calculations on calix[4]arenes also indicate strong influences of hydrogen bonds as well as of parametrizations used in different force fields: Grootenhuys, P. D. J.; Kollman, P. S.; Groenen, L. C.; Reinhoudt, D. N.; Van Hummel, G. J.; Uguzzoli, F.; Andreotti, G. D. *J. Am. Chem. Soc.* 1990, 112, 4165.

Table V.  $^1\text{H}$  NMR Shifts of Octaphenols 2-5<sup>a</sup>

	H <sup>a</sup>	H <sup>b</sup>	H <sup>c</sup>	OCH <sub>3</sub>	OH	CH <sub>3</sub>
2a	4.88 q, $^3J = 7$ Hz	6.79 (s)	6.17 (s)		8.60 (s)	1.32 d, $^3J = 7$ Hz
2b	4.36 (q)	6.39 (s)	6.23 (s)		8.73 (s)	0.75 (d)
	4.41 (q)	7.31 (s)	6.28 (s)		8.76 (s)	1.38 (d)
	4.79 (q, $^3J = 7.1$ Hz)				8.92 (s)	1.41 (d, $^3J = 7.1$ Hz)
2c	4.41 (q, $^3J = 6.9$ Hz)	6.11 (s)	6.19 (s)		8.45 (s)	1.17 (d, $^3J = 6.9$ Hz)
		6.62 (s)	6.29 (s)		8.70 (s)	
3a	4.37 (q, $^3J = 7.1$ Hz)	6.46 (s)	6.27 (s)	3.55 (s)	8.62 (s)	1.28 (d, $^3J = 7.1$ Hz)
4a <sup>b</sup>	4.47 (q, $^3J = 7.0$ Hz)	6.50 (s)	6.46 (s)	3.61 (s)		1.32 (d, $^3J = 7.0$ Hz)
5a <sup>**c</sup>	4.54 (q, $^3J = 7.0$ Hz)	7.15 (s)			8.16 (s)	1.72 (d, $^3J = 7.0$ Hz)
5b <sup>**c</sup>	4.86 (q, $^3J = 7.0$ Hz)	6.13 (s)			7.81 (s)	1.83 (d, $^3J = 7.0$ Hz)
		6.80 (s)				

<sup>a</sup>In ppm from internal TMS at 300 K; solvent DMSO-*d*<sub>6</sub> unless noted otherwise; for compound numbers, see Table I; for H numbering, see Scheme I. <sup>b</sup>At 340 K. <sup>c</sup>In acetone-*d*<sub>6</sub>.

were measured with a melting microscope.

HPLC separations were performed for the oligomer mixtures (A, B1, and B2) with Merck Lichrosphere RP18 columns (120 × 4 mm for analytical separations) with gradient elution (methanol/water). Preparative separations on similar columns of large diameter furnished only B1 as pure compound. (We thank Prof. Dr. H. Engelhardt, Mr. R. Wintringer, and Mr. H. Löw for help with HPLC separations.)

**Kinetic Experiments.** Time-concentration measurements were based on  $^1\text{H}$  NMR signal areas of the CH<sub>3</sub> groups. Several signals, e.g., those of A and B2 or B1 and rccc showed no base-line separation even at 400 MHz; the signal areas were obtained in these cases from visual comparison with computer-simulated spectra. Other CH<sub>3</sub> signals between 0.7 and 2.0 ppm also show regular concentration changes with reaction time (cf. Table III\*, supplementary material) and account for higher oligomers such as D or E.

Computer programs for the analysis of isomerizations based on integrated rate laws, as well as for numerical integration of differential rate equations corresponding to Scheme III and Table IV, were written in TURBO-PASCAL and performed on Epson 80-286 PC's equipped with mathematic coprocessor 80-287. The isomerizations were treated by a least-square computer fit of the experimental data (Figure 1); the reactions described in Scheme III were fitted by visual comparison with experimental curves (Figure 3).

**Force field calculations** with CHARMM/QUANTA from Polygen were performed on a IRIS 3130 workstation. Hydrogen bonds and electrostatics were simulated with distant dependent dielectric constants with the extreme value of 80 Debye or were suppressed by choosing arbitrarily high DC's. In almost all cases bifurcated hydrogen bonds between adjacent phenolic groups were observed (counted as 2 H bonds in Table IV). The phenolic groups are exposed to a variable degree to the solvent, which has been neglected in the calculations. For this reason, the calculated strain energies for the different compounds are of limited significance; the structural data obtained, however, are less susceptible to errors.

**Preparation of the Tetracyclophanes 2-10 (R = H). Method A (See Table I).** Resorcinol (0.1 mol; or resorcinol monomethyl ether or resorcinol dimethyl ether, respectively) was dissolved in a solution of 5 g of dried hydrogen chloride in 95 g of methanol. To this refluxing solution was added 0.1 mol of aldehyde during 30 min. The mixture was stirred for an additional 30 min; in the case using acetaldehyde, half of the solvent was distilled off. The reaction mixture was cooled to room temperature, and the precipitated macrocycles were collected, washed acid-free with water, and dried at 80 °C. Compounds 3 and 4 contained mixtures of oligomers.

For  $^1\text{H}$  NMR data, see Table V. For the purpose of analysis the phenolic calixarenes were converted to octabutyrate as described in ref 6e,f. Separation of isomers was carried out by fractional crystallization. For analytical data and melting points of butyrates, see Table I\* (supplementary material; the isomers 2a-c have melting points >360 °C under decomposition). MS: 2b (FAB) 546 (M + 1), 273 (M/2 + 1); 3a (EI) 657 (M), 328 (M/2); 4a (EI) 600 (M); 301 (M/2).

**Isolation of 2b.** 2b is the least soluble isomer of 2 and can be isolated by means of fractional crystallization from methanol. The TLC *R<sub>f</sub>* values for the three diastereomers are as follows: 2a, 0.36; 2b, 0.28; and 2c, 0.13 (in methanol, CHCl<sub>3</sub> = 5:1).

**2,8,14,20-Tetramethylcalix[4]arenoctol (2). Method B.** (The procedure based on the use of paraldehyde as described here instead of acetaldehyde leads to shorter reaction times and higher yields.) A solution of 11 g (0.1 mol) of resorcinol in 100 mL of 10% sulfuric acid was heated to 95 °C; during 1 h, 4.4 g (0.033 mol) of paraldehyde was dropped into the stirred solution. After addition, the mixture was stirred for another 0.5 h and then cooled to room temperature. The precipitate was collected and washed with water until no acid was detectable. The material was dried at 100 °C to give 13.3 g (92%) of a mixture of isomers (rccc:rctt = 3:2).

**Isolation of Intermediates of the Condensation Reaction Leading to 2.** Resorcinol (5.45 g) and 2.2 mL of paraldehyde were dissolved in 115 g of a 5% hydrogen chloride/methanol solution at 28 °C. The mixture was stirred for 30 min and then poured into a solution of 37 g of KHPO<sub>4</sub> and 7 g of NaOH in 250 mL of water. Water was added to obtain a clear solution, which was then extracted five times with diethyl ether, and the ether was distilled off. The remaining oil crystallized and contained ~90% resorcinol and 10% oligomers. The mixture of oligomers contained three main components. By use of preparative HPLC, two fractions could be isolated: a mixture of oligomers A and B1 and the pure oligomers B2.  $^1\text{H}$  NMR spectra verify the structures.  $^1\text{H}$  NMR data of A, B2, and B1 (in CD<sub>3</sub>OD;  $\delta$ ): A 1.449 (d, CH<sub>3</sub>,  $^3J = 7.2$  Hz), 4.506 (q, H<sup>a</sup>,  $^3J = 7.3$  Hz), 6.242 (s, H<sup>1</sup>, 6.221 (q, H<sup>2</sup>,  $^3J = 8.35$  Hz,  $^4J = 2.5$  Hz), 6.890 (d, H<sup>3</sup>,  $^3J = 8.0$  Hz); B2 1.440 (d, CH<sub>3</sub>,  $^3J = 7.1$  Hz), 4.495 (q, H<sup>a</sup>,  $^3J = 7.2$  Hz), 6.228 (d, H<sup>1</sup>, 6.189 (q, H<sup>2</sup>,  $^3J = 8$  Hz), 6.791 (d, H<sup>3</sup>,  $^3J = 8.3$  Hz), 6.954 (s, H<sup>4</sup>), 6.245 (s, H<sup>5</sup>); B1 1.685 (d, CH<sub>3</sub>,  $^3J = 7.4$  Hz), 4.626 (q, H<sup>a</sup>,  $^3J = 7.3$  Hz).

**Isomerization of Ring Compounds (2a-c).** rccc-2a (45 mg) and an exact amount of dioxane as internal standard (~10 mg) were dissolved in 680 mL of methanol-*d*<sub>4</sub> and brought to the appropriate temperature; the starting point of the kinetic study was the addition of 320  $\mu\text{L}$  of 4.52 M hydrogen chloride/methanol-*d*<sub>4</sub> solution. The reaction was followed by  $^1\text{H}$  NMR. For the analysis, signals of methyl groups were used, since the shift differences are greater than those of the CH<sup>a</sup> quartets and the aromatic range is partially masked by the HCl signal. Rate constants were calculated using the integrated rate laws for the case A = B = C (see Figure 1).  $^1\text{H}$  NMR (in CD<sub>3</sub>OD/HCl;  $\delta$ ): rccc 1.63 (d, CH<sub>3</sub>,  $^3J = 7.5$  Hz); rctt 1.61 (d, CH<sub>3</sub>,  $^3J = 7.4$  Hz), 1.43 (d, CH<sub>3</sub>,  $^3J = 7.2$  Hz), 0.78 (d, CH<sub>3</sub>,  $^3J = 7.3$  Hz); rctt 1.27 (d, CH<sub>3</sub>,  $^3J = 7.1$  Hz).

**Condensation Reaction to 2. Kinetic Experiments.** Resorcinol (36.6 mg) and 8 mg of dioxane were dissolved in 680  $\mu\text{L}$  of methanol-*d*<sub>4</sub> and 320  $\mu\text{L}$  of 4.52 M hydrogen chloride/methanol-*d*<sub>4</sub> solution. The mixture was brought to 300 K, and 14.8  $\mu\text{L}$  of paraldehyde were added. The reaction was followed by  $^1\text{H}$  NMR for 22 h.  $^1\text{H}$  NMR (in CD<sub>3</sub>OD/HCl;  $\delta$ ): CH<sub>3</sub>CHO(CD<sub>3</sub>)<sub>2</sub> 1.18 (d, CH<sub>3</sub>,  $^3J = 5.3$  Hz); oligomer A 1.41 (d, CH<sub>3</sub>,  $^3J = 7.2$  Hz); oligomer B1 1.65 (d, CH<sub>3</sub>,  $^3J = 7.4$  Hz); oligomer B2 1.37 (d, CH<sub>3</sub>,  $^3J = 7.2$  Hz).

**Acknowledgment.** The work in Saarbrücken was supported by the Deutsche Forschungsgemeinschaft and



the Fonds der Chemischen Industrie. F.W. thanks Professors Mann and Hauptmann, Leipzig, for advice and support.

**Registry No.** 2a, 74708-10-4; 2b, 135029-00-4; 2c, 74645-05-9; 3a, 113379-32-1; 4a, 135029-03-7; 5a, 127524-18-9; 5b, 135029-04-8; 5c, 135029-01-5; 6a, 74410-61-0; 6c, 74378-21-5; 7a, 130915-15-0; 7c, 130981-63-4; 8a, 130915-14-9; 8c, 130981-62-3; 9c, 135029-02-6; 10a, 130915-20-7; 10c, 130981-67-8; A, 612-00-0; B1, 134938-95-7; B2, 134938-96-8; resorcinol, 108-46-3; 3-methoxyphenol, 150-19-6; paraldehyde, 123-63-7; 1,2,3-trihydroxybenzoic acid, 87-66-1; 2,6-dihydroxybenzoic acid, 303-07-1; acetaldehyde, 75-07-0; benzaldehyde, 100-52-7; 2-hydroxybenzaldehyde, 90-02-8; 4-

hydroxybenzaldehyde, 123-08-0; 4-methylbenzaldehyde, 104-87-0; 2,4,6-trimethylbenzaldehyde, 487-68-3; 3-nitrobenzaldehyde, 99-61-6.

**Supplementary Material Available:** A listing of six tables (I\*, melting points and C, H, N analyses; II\*, <sup>1</sup>H NMR data for condensation products from aromatic aldehydes; III\*, <sup>1</sup>H and <sup>13</sup>C NMR data of the new stereoisomer *recci*; IV\*, contribution of higher oligomers (C, D, E) during buildup; V\*, energy contributions from CHARMM calculations for T1-T9 (of Table 4); VI\*, bond and "gable" angles for T1-T9 tetramers; graphic representations of one tetramer) (7 pages). Ordering information is given on any current masthead page.

## Studies of the Formation and Stability of Pentadienyl and 3-Substituted Pentadienyl Radicals

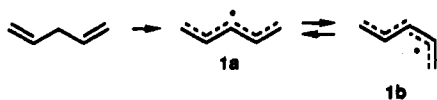
K. Brady Clark,<sup>\*,†</sup> Peter N. Culshaw,<sup>‡</sup> David Griller,<sup>†</sup> F. P. Lossing,<sup>\*,§</sup> J. A. Martinho Simões,<sup>⊥</sup> and John C. Walton<sup>\*,‡</sup>

Division of Chemistry, National Research Council of Canada, Ottawa, Ontario, Canada K1A 0R6, Department of Chemistry, University of St. Andrews, St. Andrews, Fife, KY16 9ST UK, Faculty of Science, University of Ottawa, 32 George Glinski, Ottawa, Ontario, Canada K1N 6N5, and Departamento de Engenharia Química, Instituto Superior Técnico, 1096 Lisboa Codex, Portugal

Received August 20, 1990

Pentadienyl radicals and their 3-methyl and 3-hydroxy derivatives were generated from the corresponding 1,4-pentadienes. The rates of hydrogen abstraction were studied by laser flash photolysis, and the bisallylic C-H bond dissociation energies were determined by photoacoustic calorimetry. Pentadienyl radicals were also generated by monoenergetic electron bombardment of 3-*tert*-butyl-1,4-pentadiene, and the radical's enthalpy of formation was deduced from the appearance energy of the *tert*-butyl cation. Evaluation of all recent data leads to recommended values of  $\Delta H_f^\circ(\text{pentadienyl}) = 49.8 \pm 1.0 \text{ kcal mol}^{-1}$  and  $\text{DH}^\circ((\text{CH}_2=\text{CH})_2\text{CH}) = 76.6 \pm 1.0 \text{ kcal mol}^{-1}$ . The EPR spectra of 3-methylpentadienyl and several other radicals were also examined. The effect of substituents on the stabilization energy of pentadienyl radicals was assessed, and pentadienyl radicals were compared with other delocalized polyenyl radicals.

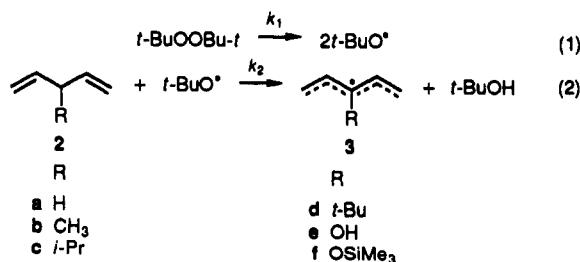
Alkenes,  $\text{RCH}_2\text{CH}=\text{CH}_2$ , frequently undergo scission of the allyl C-H bond in homolytic reactions. These bonds are weaker than the secondary C-H bonds in alkanes because the allylic radicals  $\text{RCH}\dot{\text{C}}\text{HCH}_2$  are thermodynamically stabilized by delocalization of the unpaired electron over three carbon centers. The enthalpy of formation of the allyl radical is known to good precision, and there is considerable information about the effects of substituents.<sup>1</sup> Hydrogen abstraction from "skipped" dienes, e.g., 1,4-pentadiene, by free radicals leads to the formation of pentadienyl radicals, 1, in which the unpaired electron is delocalized over five carbon centers. These types of intermediate are important in many processes including hydrocarbon combustion and unsaturated fatty acid (and lipid) autoxidation. Because of the greater extent of electron delocalization, 1 is more thermodynamically stabilized than allyl. In spite of several attempts to quantify



the difference<sup>1-4</sup> in stabilization energies, the enthalpy of formation of 1,  $\Delta H_f^\circ(\text{PD}^\bullet)$ , is known with rather poor

precision and practically nothing is known about the effect of substituents on this quantity or on the closely related stabilization energy (SE) of this type of radical.

We have studied the formation of radical 1 and several 3-substituted pentadienyl radicals. In order to obtain data that were as reliable as possible, we used three independent methods to determine the enthalpies of formation. Firstly, pentadienyl radicals were generated by hydrogen abstraction from the corresponding 1,4-pentadiene, and the C(3)-H BDE was then measured using photoacoustic calorimetry.<sup>4</sup> Secondly, pentadienyl radicals were generated



by electron bombardment of the 3-*tert*-butyldiene 2d in a mass spectrometer.<sup>5</sup>  $\Delta H_f^\circ(\text{PD}^\bullet)$  was then deduced from

(1) McMillen, D. F.; Golden, D. M. *Annu. Rev. Phys. Chem.* 1983, 33, 493.

(2) Trenwith, A. B. *J. Chem. Soc., Faraday Trans. 1* 1980, 76, 266; *Ibid.* 1982, 78, 3131.

(3) Walton, J. C. *Rev. Chem. Intermed.* 1984, 5, 249.

(4) Burkey, T. J.; Majewski, M.; Griller, D. *J. Am. Chem. Soc.* 1986, 108, 2218.

<sup>†</sup> National Research Council of Canada. Issued as NRCC publication No. 32852.

<sup>‡</sup> St. Andrews University.

<sup>§</sup> Ottawa University.

<sup>⊥</sup> Instituto Superior Técnico Lisboa.